Journal of Research in Pharmacy

Research Article

www.jrespharm.com

Cilnidipine nanocrystals; Formulation, characterization and bioavailability study

Suray A. HAZZAA [1], Nawal A. RAJAB [2 *]

[1] Department of Pharmacy, Anbar Health Directorate, Anbar, Iraq.
[2] Department of Pharmaceutics, College of Pharmacy, University of Baghdad, Baghdad, Iraq.
* Corresponding author: dr.nawalayash@copharm.uobaghdad.edu.iq (N.R.) Tel: +964-771-986 82 77.

Received: 8 January 2024 / Revised: 14 February 2024 / Accepted: 16 February 2024

ABSTRACT: Cilnidipine a fourth generation calcium channel blockers, it was utilized to reduce cardiovascular events. Since cilnidipine is a material classified as Biopharmaceutics Classification System (BCS) Class-II, which is extremely poorly soluble and has a high permeability in turn low bioavailability. Thus, by employing solvent anti-solvent technology, cilnidipine (CLD) can be produced as nanocrystals (NCs). Getting beyond those obstacles could boost the material's solubility and bioavailability. A pair of distinct stabilizers (Soluplus® and Tween20) in a ratio of CLD: Soluplus : Tween20 (1:0.25:0.5) were used to prepare cilnidipine nanocrystals (CLD NCs). Rats were used to evaluate and assess the pharmacokinetics in vivo parameters of CLD and CLD NCs. The optimal formula that was created revealed 62.1 nm with 0.18, which represent particle size and polydispersity index (PDI), respectively. At 6 minutes, 99% of CLD NCs were released in phosphate buffer 6.8. It is evident that CLD NCs had a higher relative bioavailability by around 3.17 times and that their area under the concentration time curve (AUC) and C_{Pmax} were greater than those of bulk CLD. Additionally, the CLD NCs' Tmax was lower than that of the CLD pure medication. Accordingly, it was evident from the observed pharmacokinetic parameters (AUC, CPmax, and Tmax) that the CLD NCs enhanced the the oral bioavailability of CLD in rats.

KEYWORDS: Cilnidipine; Soluplus; Nanocrystals; Tween20; solvent anti-solvent.

1. INTRODUCTION

The bioavailability issue of medications that are poorly water-soluble has long been a significant task in the pharmaceutical industry. Lately, "Nanotechnology" has been increasingly important and widely used in the modern pharmaceutical industry. Pharmaceutical nanoparticles are those that are less than one micrometer in size, have a solid structure, and typically range in size from 1 to 1000 nm [1]. By reducing the particle size, nanoparticles increase surface area, which improves water solubility, dissolution rate, and bioavailability. Additionally, nanoparticles can be designed as prolonged, controlled release, site-specific drug delivery systems that lower drug toxicity and adverse effects [2, 3]. Nanoparticles come in a variety of forms, including lipid nanoparticles, polymeric nanoparticles, and nanosuspension [4].The two main techniques for making nanomaterials are the top-down method and the bottom-up method. Without utilizing organic solvents, top-down approaches reduce the size of the large drug particle to a small size. Both media milling and high-pressure homogenization are names for both procedures [5] The drug precipitates because of its low water solubility when the medication is dissolved in a mixture of an organic solvent system, such as methanol, and a miscible anti-solvent system, such as water [6].

Cilnidipine, a fourth-generation calcium channel blocker, was utilized to reduce cardiovascular events. Since cilnidipine is a material classified as BCS Class-II, which is extremely poorly soluble and has a high permeability and, in turn, low bioavailability, Therefore, cilnidipine (CLD) can be developed as nanocrystals (NCs) to improve the dissolution rate and bioavailability by using solvent-anti-solvent technology, in the sense that, in spite of very low adherence, CLD is an option for hypertension and vascular problems associated with hypertension. The use of nanoparticle engineering approaches to improve medication solubility and dissolution rates has been advocated for pharmaceutical purposes. For example, to enhance the oral bioavailability of medications that are not soluble in water and to hasten the rate of drug dissolution, as an example, the implementation of nanosizing techniques boosted the surface area of

How to cite this article: Hazzaa SA, Rajab NA. Cilnidipine nanocrystals; Formulation, characterization and bioavailability study. J Res Pharm. 2024; 28(6): 2057-2067.

ISSN: 2630-6344

http://dx.doi.org/10.29228/jrp.881

medication. More valuable interaction with the solvent is made possible by a large surface area, which raises solubility [7]. According to this, drug particles with nanocrystal surfaces should be bound with stabilizers that are part of the nanocrystal formulation. and cause the steric stabilization to take place. The physicochemical properties of the polymer being employed and the loaded polymer determine the appropriate formulation method for nanocrystals. Nonetheless, the capacity of nanocrystals to combine the bioavailability and rate of dissolution of poorly soluble medications is a benefit [8, 9]. CLD is a BCS Class II medication with a poor dissolving rate and low water solubility; it possesses a log P value of 4.7 and a strong lipophilic nature and also has good intestinal permeability. However, only 13% of CLD is bioavailable orally in humans [10]. Low oral bioavailability of CLD is thought to be primarily caused by low water solubility, a slow dissolution rate, and high liver first-pass metabolism [11]. CLD is regarded as being relatively more effective and safe than the other calcium antagonists in the therapy of hypertension, despite its low oral absorption qualities [12].

2. RESULTS

Particle size analysis of lyophilized CLD NCs, as shown in Figure 1, was performed using the Malvern Panalytical to analyze the CLD NC samples. As indicated in Table 1, particle size and PDI were examined separately. The particle size distribution of nanoparticles from a particle analyzer is represented by measurements called the particle size distribution (PDI).

Table 1. CLD NCs Size and PDI before and after Lyophilization

Formula name	Before lyophilization		After lyophilization	
	Particle size(nm)	PDI	Particle size(nm)	PDI
CLD NCs	53.3±2.1	0.14±0.06	62.1±1.7	0.18±0.03

2.1. Study of in vitro dissolution

The profile of dissolution for pure CLD in phosphate buffer 6.8 and CLD NCs is depicted in Figure 2. Using the similarity factor f2, the dissolution characteristics of the CLD NCs formula and the pure medication used as a reference were compared. The similarity factor f2 statistical analysis indicates that CLD NCs have a f2 value of 6.003.

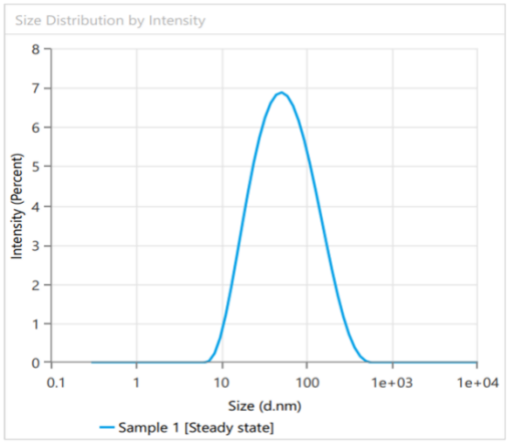

Figure 1. Chart of particle size distribution of optimized CLD NCs

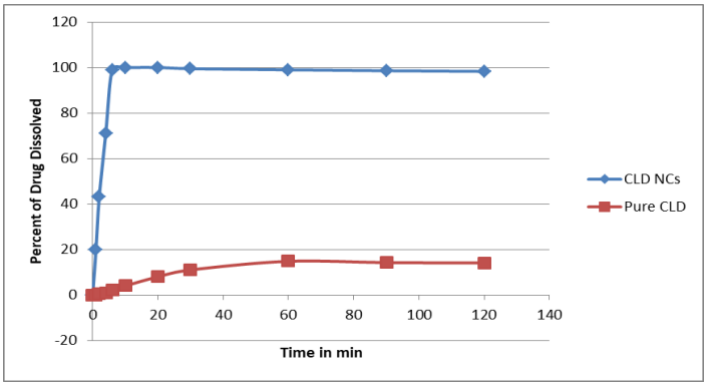

Figure 2. Prepared CLD NCs and pure CLD in phosphate buffer 6.8: An in-vitro dissolution profile

2.2. Fourier Transform Infrared (FTIR) Spectroscopy

Additionally, the potential for chemical interactions between the medication and stabilizers was screened using FT-IR spectroscopy. Figures 3, 4, and 5 show the FT-IR spectra of pure CLD, physical mixes, and CLD NCs, respectively. The FTIR absorption peaks were evaluated.

Journal of Research in Pharmacy
Research Article

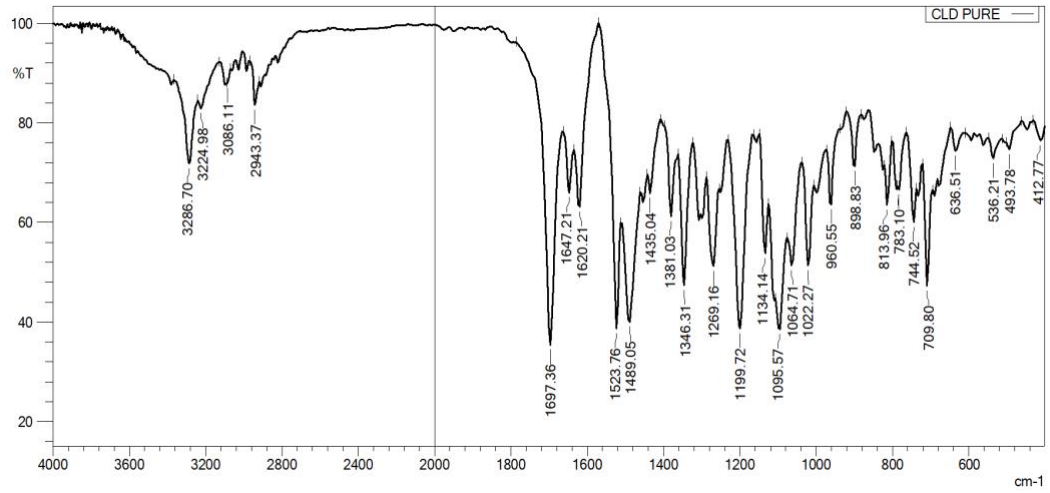

Figure 3. Pure CLD's FTIR spectra

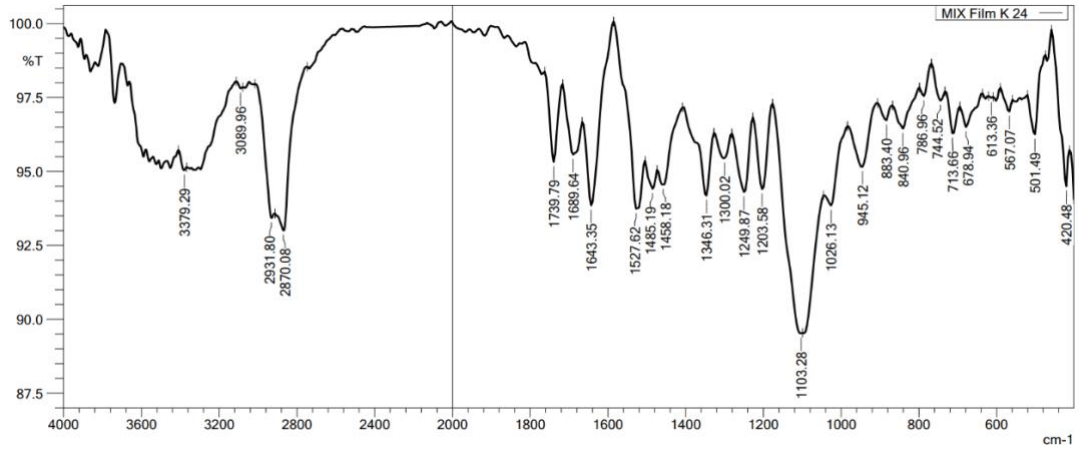

Figure 4. The physical mixture's FTIR spectrum for CLD NCs

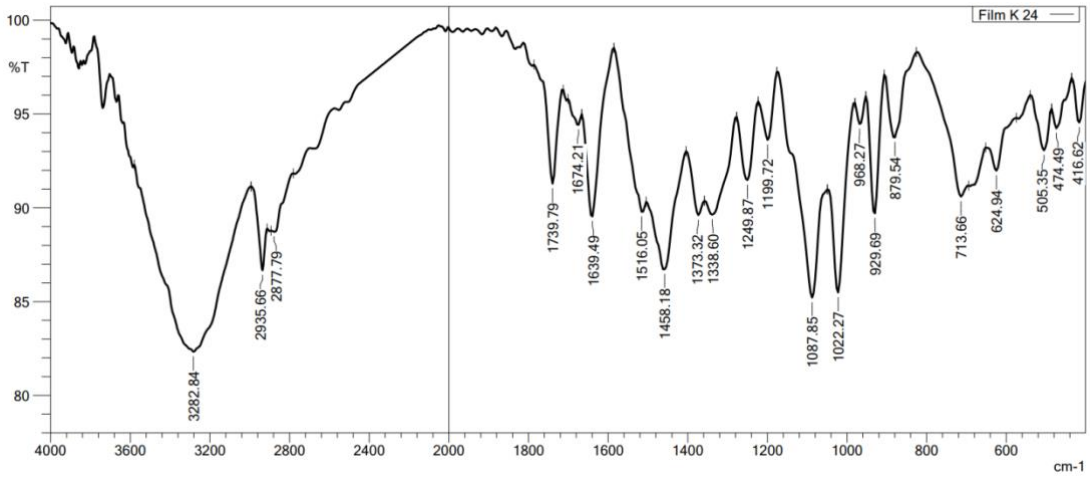

Figure 5. FTIR spectra of CLD NCs that are optimized

2.3. X-ray powder diffractometry (XRPD)

Figures 6, 7, and 8 depict the outcomes of the XRPD patterns obtained from the X-ray diffractometer for bulk CLD, physical mixture, and CLD NCs lyophilized powder.

2.3.1. Spiked plasma samples calibration curve

Using the suggested method for the plasma that had been spiked with a standard solution containing a known quantity of CLD, the calibration curve was obtained. The HPLC study's findings, as shown in Figure 9, To determine CLD in samples of spiked plasma and standard solutions for the mobile phase, the approach was exact, focused, and sensitive. As shown in Figures 9, 10, 11, and 12, the developed calibration curve is demonstrated in Figure 12.

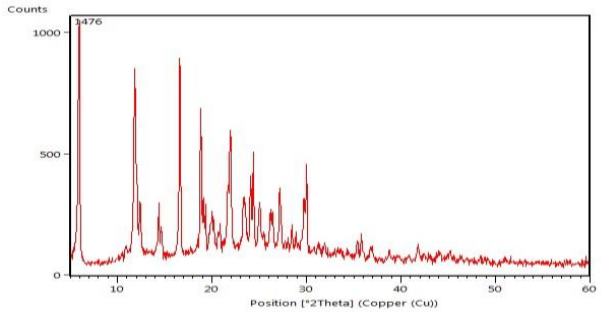

Figure 6. PXRD chart for pure CLD

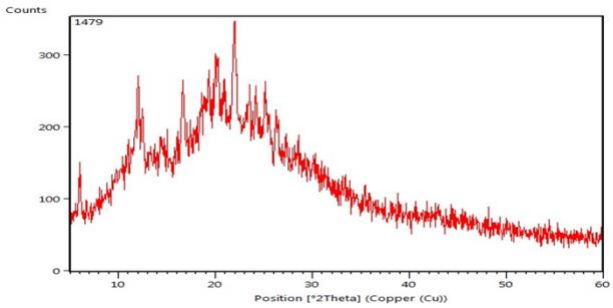

Figure 7. PXRD chart for physical mixture of optimized CLD NCs

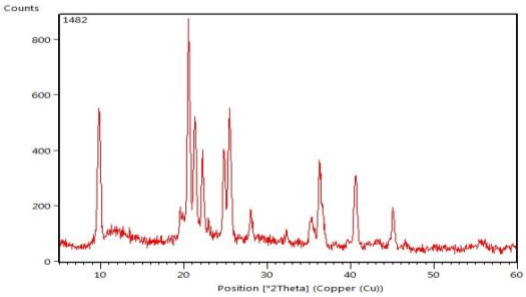

Figure 8. PXRD Chart for Optimized CLD NCs

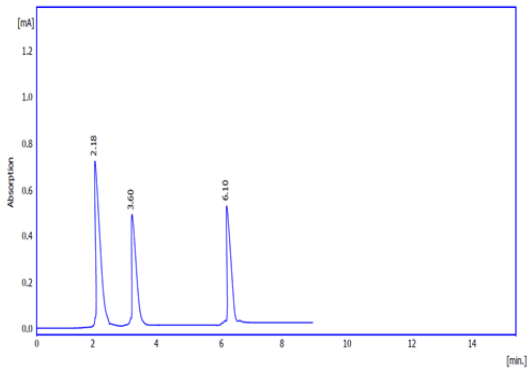

Figure 9. Samples of spiked plasma calibration curve with constant internal standard (IS) concentration (10 ng/ml) and mobile phase containing CLND.

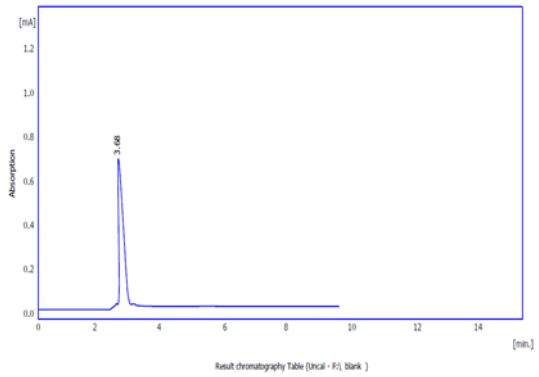

Figure 10. A blank plasma chromatogram

Journal of Research in Pharmacy
Research Article

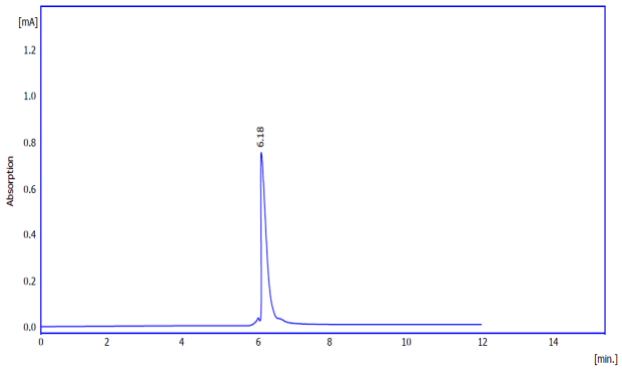

Figure 11. Chromatograms for CLD

2.4. *In vivo* pharmacokinetics

To calculate and assess the in vivo pharmacokinetics of CLD and CLD NCs, rats were employed. Table 2 lists the key pharmacokinetic parameters and plots the CLD plasma concentration-time profile. Furthermore, the Tmax of the CLD NCs was lower than that of the CLD pure drug, as seen in Figure 14. Consequently, the oral bioavailability of CLD in rats appeared to be optimized by the formulation of CLD NCs as obtained by the recognized pharmacokinetic studies [13] .

Table 2. The pharmacokinetic Parameters for Pure CLD and CLD NCs

Parameter	Pure CLD	CLND NCs
C $_{max(ng)}$	2±0.16	133±1.8
T $_{max}$ h	1	0.75
T ½ h	2.3±0.15	2.0±0.13
AUC $_{0\rightarrow12}$	247.6± 11	796.505±18
AUC $_{0\rightarrow\infty}$	276.5 ± 14	876.505± 27

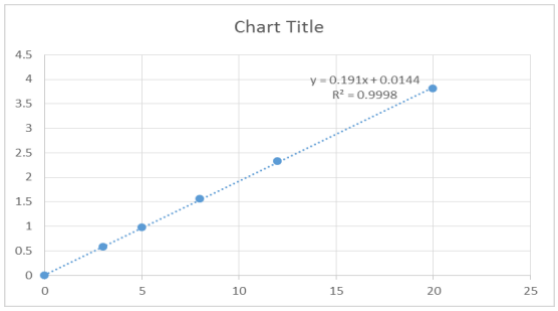

Figure 12. Spiked calibration curve for CLD

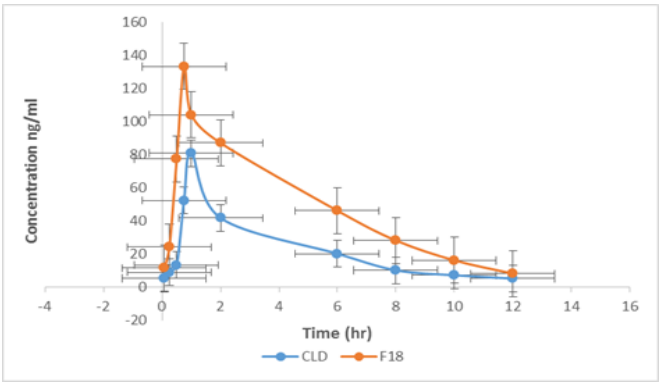

Figure 13. Rat plasma concentration-time curves following oral CLD and CLDNC therapy (mean ± SD).

http://dx.doi.org/10.29228/jrp.881
J Res Pharm 2024; 28(6): 2057-2067

3. DISCUSSION

3.1. Analysis of the prepared CLD NCs

3.1.1. Evaluation of the polydispersity index (PDI) and particle size

The CLD NCs samples were analyzed using the Malvern Panalytical particle size analyzer. and it displayed that the optimized formula results were 53.3 nm with 0.14, which represent particle size and PDI, respectively. The particle size analysis of lyophilized CLD NCs (Figure 2) displayed that the size was still in the nanorange below 100 nm after lyophilization (62.1 nm) with a PDI of 0.18, as displayed in Table 1. The variable that depicts the distribution of nanoparticles is called the PDI. The particle size distribution's variation, spread, and breadth are measured by the PDI, which serves as a stand-in for the nanosuspension's long-term stability. Although the PDI value of monodisperse samples is lower than that of polydisperse samples, higher PDI values indicate a wider particle size dispersion, indicating the sample's polydisperse nature. Values between 0 and 0.05 are regarded as "monodisperse standards," between 0.05 and 0.08 as "nearly monodisperse," between 0.08 and 0.7 as "mid-range polydispersity," and beyond 0.7 as "very polydisperse." Tween 20 was adsorbed at specific locations on the top layer of freshly produced drug particles [14], as a result, it prevents further growth by preventing the insertion of drug molecules from solutions into crystal lattices, which led to the production of the previously described nanosized particles with nanorange.

3.1.2. In vitro dissolution study

As shown in Figure 3, the CLD NCs exhibited a notably elevated rate of dissolution in nanosuspension form, with over 70% of the CLD being liberated within 5 minutes. Because of the increased particle surface area resulting from the reduction of particle size, CLD NCs dissolve more quickly; hence, after 6 minutes, about 99% of CLD NCs were released as opposed to 2.2% of pure CLD in phosphate buffer 6.8. It makes sense that tween 20 had a better dissolving rate and wettability of CLD particles. The reason for such a result is mainly attributed to the Noyes-Whitney equation, which declares that enhancing the dissolution rate is accompanied by particle size reduction caused by a large surface area and then enhancing the wettability and contact of nanoparticles with the dissolution medium. The amphiphilic nature of solupus might also enhance the surface wettability of the low-water-soluble CLD, resulting in a faster release of CLD through nanocrystal formulation [15,16]. Using the similarity factor f2 to compare the dissolution characteristics of the CLD NCs formula and pure CLD powder, which is used as a reference, when f2 is greater than 50, it is claimed that two dissolution profiles are comparable, while if f2 is less than 50, this indicates that there are differences in the solubility profiles of CLD NCs and pure CLD powder [17]. A statistical analysis using the similarity factor (f2) revealed that CLD NCs had a superior release profile over pure CLD (f2 = 6.003). The minimizing of CLD crystallinity towards an amorphous nature leads to an elevation in internal energy and molecular motion, which may assist in reinforcing the rate of dissolution [18].

3.1.3. Fourier Transform Infrared (FTIR) Spectroscopy

Additionally, the potential for chemical interactions between the medication and stabilizers was observed using FT-IR spectroscopy. Figures 4, 5, and 6 show the FT-IR spectra of pure CLD, physical mixes, and CLD NCs, respectively. The FTIR absorption peaks for the pure CLD were seen at 3286 cm^{-1} and 1697 cm^{-1} for the stretching of the N-H vibration, 1647 cm-1 and 1620 cm-1 for the stretching of the C=O vibration, 1523 cm-1 and 1346 cm^{-1} for the stretching of the NO2 vibration, and 1134 cm^{-1} and 1623 cm^{-1} for the stretching and deformation of the -O-CH3 vibration, as appeared in Table 3. All of the physical blends and CLD NCs both displayed distinctive CLD peaks. The majority of the CLD peaks were maintained, and there was no noticeable shift in wave number or any significant disappearances in the spectrum, which further demonstrated the high compatibility of medications and excipients and the lack of any discernible interactions between the functional groups of CLD and stabilizers [19].

Table 3. FTIR spectrum of chemical groups of CLD [19].

Theoretical values wave number (cm-1)	Chemical group	Theoretical values wave number (cm-1)	Chemical group
3286	N–H stretching vibration	1523 and 1346	NO2 stretching
1697	C=O stretching	1134 and 1623	O-CH3 deformation vibration and stretching
1647 and 1620	C=C stretching		

3.1.4. X-ray powder diffractometry (XRPD)

Differential peaks were visible at two scattered angles of 11.8°, 16.43°, 19.77°, 21.72°, and 23.21° on the XRD chart of pure CLD, showing its crystalline nature as shown in Figure 7. Additionally, the characteristic diffraction peaks of bulk CLD were also obtained using the physical mixtures as shown in Figure 8, and a possible dilution effect was indicated by a slight reduction in the intensity of the CLD peak. This suggests that the mixing process had no impact on the crystalline structure of CLD, while in the case of CLD NCs XRD chart compared to pure CLD, the locations of the most identifiable crystalline peaks were unchanged, but the peak intensities were lower, and the amorphous patterns were established. This would have resulted from the preparation-related decrease in particle size, and it provided evidence of the transformation of CLD into an amorphous state in the form of nanocrystals, as seen in Figure 9 [20] .

3.1.5. A spiked calibration curve for samples of plasma

Using a standard solution with a known concentration of CLD and the suggested protocol for the spiked plasma, the calibration curve was produced. As a result of the High-Pressure Liquid Chromatography experiment, the technique for detecting CLD in mobile phase standard solutions and spiked plasma samples proved to be focused, sensitive, and accurate; Figure 10 illustrates the free overlapping of endogenous components with the blank plasma chromatogram. The spiked plasma chromatogram, which is displayed in Figures 10, 11, 12, and 13, shows that CLD was completely separated from the internal standard (IS) nimodipine, which produced a peak at 2.18 minutes with a retention time (Rt) of 6.18 minutes. The derived calibration curve, shown in Figure 13, illustrates a linear relationship between the concentration of CLD and the relative peak area of CLD to nimodipine. The amount of CLD in animal blood was calculated using the HPLC method, and all validation parameters fell within acceptable bounds. CLD was computed correctly when HPLC-validated parameters were used. The duration of retention was 6.1 minutes. To determine the lowest limit of quantification, which was 5 µg/ml, and to estimate the linearity of the procedure, five concentrations were used [21]

3.1.6. In vivo pharmacokinetics

Table 2 summarizes the key pharmacokinetic parameters. It is evident that CLD NCs had a higher relative bioavailability and CPmax than bulk CLD, with the former being about 3.17 times higher. Furthermore, as Figure 14 illustrates, the Tmax of the CLD NCs was shorter than that of the CLD pure drug. AUC0→∞ was 276.5 for CLD and 876.505 for CLD NCs; therefore, the established pharmacokinetic results clearly showed that the formulation of CLD NCs was capable of enhancing the oral bioavailability of CLD in rats [22]. According to these findings, a number of factors contributed to the CLD NCs' oral bioavailability enhancement: First, due to the solubilization impact of Soluplus [23].

Since the particle size reduction of CLD NCs facilitated the optimization of oral bioavailability as a sequence for improvement in solubility and in vitro rate of dissolution, Second, when CLND NCs cross the intestinal biological barriers and enter the circulatory system, they significantly increase the permeability of their membrane by increasing the surface area of contact between them and the barriers [24].

4. CONCLUSION

In accordance with the findings, the optimized formula for CLD NCs as nanocrystals in a ratio of CLD: Soluplus: Tween20 (1:0.25:0.5) showed enhanced dissolution profile and improvement in pharmacokinetic parameters, especially relative bioavailability, whereas a 3.17-fold increment was attained when CLD NCs were administered as compared to pure CLD.

5. MATERIALS AND METHODS

Hyperchem Chemical Co., Ltd. (China) provided Tween20, Soluplus®, and Cilnidipine powder (CLD). The grade of all other chemicals and solvents was that of analytical reagents.

5.1. Cilnidipine Nanocrystal Fabrication

To dissolve ten milligrams of CLD, the organic liquid methanol was used in five milliliters. On the other hand, as table 4 shows, the anti-solvent system is made up of 50 mL of deionized water mixed with

CLD stabilizers (Tween20 and Soluplus®) at a ratio of 1:0.25:0.5, meaning that the medication is mixed with the stabilizers. The next step is to gradually add an organic solvent to an aqueous solution using a syringe pump while a hotplate magnetic stirrer at room temperature is utilized to mechanically agitate the mixture at a speed of 1000 rpm [25]. Following that, to get the desired results and allow the methanol to evaporate, the sample was stirred for an hour at a temperature of 25 ^{o}C [26]. Every sample is subjected to sonication for six minutes (three seconds of on and one second of off) employing an ultrasonic probe powered by 60 watts. Waves were sent downhill and back upward through the probe, which was submerged in the liquid 10–12 mm below the surface. The probe's tip diameter was 8 mm. The temperature of the liquid was also adjusted during ultrasonication by utilizing an ice water bath.

Table 4. Prepared Formulas for CLD Nanocrystals

Ingrediants	Amount
CLND	10 mg
Soluplus	2.5 mg
Tween 20	5 mg
Methanol	5ml
D W	50 ml

5.2. Evaluation of the fabricated nanocrystals: Particle Size and the Polydispersity Index (PDI)

The polydispersity index and particle size have been determined or evaluated using the Malvern Mastersizer 2000 MS (Worcestershire, Great Britain), wherein the quantity of light that the sample's molecules dynamically scatter is quantified as a function of time at a steady temperature of 25 °C and a scattering angle of 90 degrees. Two or three milliliter samples of the nanosuspension were picked in order to find the polydispersity index and particle size. Sometimes prepared diluted solutions are combined with simple ultrasonication to aid in the separation of loosely held agglomerates [27] .

5.3. Freeze-drying of nanosuspensions

For additional evaluation, the resultant compound was dried after being frozen to produce a dry powder for further analysis. A dry powder was obtained by freeze-drying 100 mL of the best-chosen formula for an entire day, using 3% w/v cryoprotectant mannitol. Next, four containers were placed in a deep freezer and frozen at -60 ^{o}C. After the frozen flasks were joined to the apparatus's vacuum port, four flasks, each carrying 100 mL of nanosuspension, were connected, and the device was run until dry powder was created. 48 hours are needed for the solvent sublimation of frozen samples [28, 29].

5.4. Fourier Transform Infrared (FTIR) Spectroscopy

The Fourier transform infrared spectroscopy (FTIR) Shimadzu 8300 Japan was used to acquire the FTIR spectra. Potassium bromide was used to compress samples of the chosen formula's CLD NCs, Soluplus®, mannitol, and tween 20. The obtained spectra have a wavenumber of 4000-400 cm^{-1} [18].

5.5. Analysis using X-ray powder diffraction (XRPD)

A continuous scan covering 5-80 degrees was conducted employing the XRD-6000, Shimadzu, Japan, to analyze the patterns of both pure and nanocrystal cilnidipine. 0.050° (2θ) was selected as the scan step size, 60 seconds was selected as the scan step time, 40 kV was the operating voltage, and 30 mA was the current [30].

5.6. The lyophilized cilnidipine nanocrystals' in-vitro dissolution profile

A type II dissolution apparatus was used to conduct an in-vitro dissolution test on lyophilized CLD powder. A precisely determined amount of lyophilized powder, equivalent to 10 mg of CLD, was added to 900 ml of phosphate buffer pH 6.8, which served as the dissolve medium. The device rotated at 100 rpm at 37 °C. During each of the three experiment runs, an aliquot of five milliliter samples was removed at regular intervals (1, 2, 5, 10, 15, 20, 30, 60, 90, and 120 minutes) and replaced with new dissolving media. After passing the samples through a 0.45µm filter syringe, a UV spectrometer was used to test the samples spectrophotometrically. The outcomes of the dissolution experiments were statistically confirmed by applying a f2 similarity factor. Similar dissolution characteristics were taken into account using f2 (equation No. 1 below).

Journal of Research in Pharmacy
Research Article

$$f_2 = 50 \log \left\{ \left[1 + \frac{1}{n} \sum_{n=1}^{n} (R_t - T_t)^2 \right]^{-0.5} * 100 \right\} \quad \text{----------1}$$

where (n) is the total number of time points for dissolution. The reference and test dissolution values at t time are (Rt), (Tt), respectively. When f2 values are larger than 50 (50–100), the two dissolution profiles are considered similar, or else the profiles are not identical [31].

5.7. Animal experiments

The techniques used to evaluate the parameters affecting bioavailability were in accordance with the recommendations issued by representatives of the National Committee on Science and Technology Research Ethics (NENT, Norway). Abdulqader and Rajab 2023, weighing 200 ±20 grams, each male Wistar rats (n = 12) were employed to measure the bioavailability characteristics. They were divided equally between two groups of six rats. Except for being allowed to drink water before the trail, all groups had to fast for twelve hours [32]. To obtain CLD NCs at a concentration of 0.25 mg/mL, 40 mL of deionized water have been mixed with 10 mg of CLD NC powder. Next, using a gavage tube, the rats received an oral dose of 2.0 mg/kg for both the CLND NC dispersion and the CLD dispersion powder, as depicted in figure 1. Before being taken orally, each sample was shaken for five minutes to ensure complete dispersion. Blood samples (0.5 mL) were taken in the retroorbimtal venous plexus at 5, 15, 30, 45 minutes, 1.0, 2.0, 6.0, 8.0, 10.0, and 12.0 hours after distribution. Next, tubes containing EDTA were used to hold blood samples in a microcentrifuge and centrifuged right away in a cool centrifuge for 15 minutes at 4500 revolutions per minute. After that, the samples were stored at -25 °C until the HPLC analysis was performed [10]. The study was carried out in accordance with the Declaration of Helsinki, the code of ethics of the World Medical Association.

5.8. Bioanalytical Technique

The deproteinization procedure was used to determine the CLD of the rat plasma sample. 100 microliters of melting plasma, 500 microliters of acetonitrile, and ten microliters of an internal standard solution (methanol-solubilized 200 ng/mL nimodipine) were combined in order to precipitate protein. An Ohaus cooling centrifuge was used to rotate the mixture for ten minutes at 8,000 rpm after it had been stirred for five minutes. After filtering the collected supernatant using a 0.22 µm filter syringe, 20 µL of the filtered liquid was introduced into the HPLC system for analysis. Up to 70% acetonitrile and 30% ammonium acetate solution are present in the mobile phase, which runs at a rate of 0.3 mL/min. The same process is used to extract plasma samples in the event that a CLD with an unknown concentration is found in the rat plasma obtained throughout the test. The plasma sample is then spiked with 100 µl of mobile phase containing a 5 µg/ml internal standard (nimodipine). The equation derived from the spiked calibration curve might be used to compute the unknown concentration of CLD. Following time-dependent measurements of the plasma concentration of CLD, the analysis employs a non-compartmental approach to determine pharmacokinetic parameters using PK-SOLVER. The drug's half-life (T1/2), time maximum (tmax), and CPmax of the plasma concentration-time curve's area (AUC0–24) are the areas under the curve from 0 to 24 hours [33].

Figure 14. Administration of an oral CLND NCs solution

5.9. Statistical analysis

The mean values (mean±SD; n = 3) were displayed for the results. A difference was deemed statistically significant when the significance level was less than 0.05. Using a student t-test, the Cmax, Tmax, AUC0-24, and AUC0-∞ pharmacokinetic parameters were statistically investigated [34, 35].

Acknowledgment: The authors are extremely grateful to college of pharmacy, university of Baghdad and to department of pharmaceutics for their generously offered all available tools required to complete this task.

Author contributions: Concept – N.R.; Design – S.H., N.R.; Supervision – N.R.; Resources – S.H.; Materials – S.H.; Data Collection and/or Processing – S.H.; Analysis and/or Interpretation – S.H., N.R.; Literature Search – S.H., N.R.; Writing – S.H.; Critical Reviews – N.R.

Conflict of interest statement: "The authors declared no conflict of interest" in the manuscript.

REFERENCES

[1] Al-lami MS, Oudah MH, Rahi FA. Preparation and characterization of domperidone nanoparticles for dissolution improvement. Iraqi J Pharm Sci. 2018;27(1):39-52. https://doi.org/10.31351/vol27iss1pp39-52

[2] Shukr MH, Ismail S, Ahmed SM. Development and optimization of ezetimibe nanoparticles with improved antihyperlipidemic activity. J Drug Deliv Sci Technol. 2019;49:383-395. http://dx.doi.org/10.1016/j.jddst.2018.12.001

[3] Arora D, Khurana B, Rath G, Nanda S, Goyal AK. Recent advances in nanosuspension technology for drug delivery. Curr Pharm Des. 2018;24(21):2403-2415. https://doi.org/10.2174/1381612824666180522100251

[4] Rashid AM, Abd-Alhammid SN. Formulation and characterization of itraconazole as nanosuspension dosage form for enhancement of solubility. Iraqi J Pharm Sci. 2019;28(2):124-133. https://doi.org/10.31351/vol28iss2pp124-133

[5] Azimullah S, Sudhakar C, Kumar P, Patil A, Usman MRM, Usman MZS, Jain BV. Nanosuspensions as a promising approach to enhance bioavailability of poorly soluble drugs: An update. J drug deliv Ther. 2019;9(2):574-582. https://doi.org/10.22270/jddt.v9i2.2436

[6] Rathore SK, Pathak BK. Formulation and evaluation of aceclofenac-loaded nanoparticles by solvent evaporation method. Res J Pharm Dosage Forms and Tech. 2020;12(4):237-244. https://doi.org/10.5958/0975-4377.2020.00039.7

[7] Alhagiesa AW, Ghareeb MM. The Formulation and characterization of nimodipine nanoparticles for the enhancement of solubility and dissolution rate. Iraqi J Pharm Sci. 2021;30(2):143-152. https://doi.org/10.31351/vol30iss2pp143-152

[8] Thapa RK, Kim JO. Nanomedicine-based commercial formulations: Current developments and future prospects. J Pharm Investig. 2023;53(1):19-33. https://doi.org/10.1007%2Fs40005-022-00607-6

[9] Hussien RM, Ghareeb MM. Formulation and characterization of isradipine nanoparticle for dissolution enhancement. Iraqi J Pharm Sci. 2021;30(1):218-225. https://doi.org/10.31351/vol30iss1pp218-225

[10] Diwan R, Ravi PR, Pathare NS, Aggarwal V. Pharmacodynamic, pharmacokinetic and physical characterization of cilnidipine loaded solid lipid nanoparticles for oral delivery optimized using the principles of design of experiments. Colloids Surf B Biointerfaces. 2020;193:111073. https://doi.org/10.1016/j.colsurfb.2020.111073

[11] Rao MRP, Kulkarni S, Sonawane A, Sugaonkar S. Self-nanoemulsifying drug delivery system of cilnidipine. Indian J Pharm Educ Res. 2021;55(3):664-676. http//doi.org/10.5530/ijper.55.3.138

[12] Chakraborty RN, Langade D, More S, Revandkar V, Birla A. Efficacy of cilnidipine (L/N-type Calcium Channel Blocker) in treatment of hypertension: A meta-analysis of randomized and non-randomized controlled trials. Cureus. 2021;13(11):e19822. https://doi.org/10.7759/cureus.19822

[13] Hu Q, Fu X, Su Y, Wang Y, Gao S, Wang X, Xu Y, Yu C. Enhanced oral bioavailability of koumine by complexation with hydroxypropyl-β-cyclodextrin: Preparation, optimization, ex vivo and in vivo characterization. Drug Deliv. 2021;28(1):2415-2426. https://doi.org/10.1080/10717544.2021.1998248

[14] Khan FU, Nasir F, Iqbal Z, Neau S, Khan I, Hassan M, Iqbal M, Ullah A, Khan SI, Sakhi M. Improved ocular bioavailability of moxifloxacin HCl using PLGA nanoparticles: Fabrication, characterization, in-vitro and in-vivo evaluation. Iran J Pharm Res. 2021;20(3):592. https://doi.org/10.22037%2Fijpr.2021.114478.15054

[15] Shaker MA, Elbadawy HM, Al Thagfan SS, Shaker MA. Enhancement of atorvastatin oral bioavailability via encapsulation in polymeric nanoparticles. Int J Pharm. 2021;592:120077. https://doi.org/10.1016/j.ijpharm.2020.120077

[16] Gigliobianco MR, Casadidio C, Censi R, Di Martino P. Nanocrystals of poorly soluble drugs: drug bioavailability and physicochemical stability. Pharmaceutics. 2018;10(3):134. https://doi.org/10.3390/pharmaceutics10030134

[17] Kadhim ZJ, Rajab NA. Formulation and characterization of glibenclamide nanoparticles as an oral film. Int J Drug Deliv Technol. 2022;12(1):387-394. http://dx.doi.org/10.25258/ijddt.12.1.70

[18] Abbas IK, Rajab NA, Hussein AA. Formulation and in-vitro evaluation of darifenacin hydrobromide as buccal films. Iraqi J Pharm Sci. 2019;28(2):83-94. https://doi.org/10.31351/vol28iss2pp83-94

[19] Liu Q, Mai Y, Gu X, Zhao Y, Di X, Ma X, Yang J. A wet-milling method for the preparation of cilnidipine nanosuspension with enhanced dissolution and oral bioavailability. J Drug Deliv Sci Technol. 2020;55:101371. https://doi.org/10.1016/j.jddst.2019.101371

[20] Mohana M, Vijayalakshmi S. Development and characterization of solid dispersion-based orodispersible tablets of cilnidipine. Beni-Suef Univ J Basic Appl Sci. 2022;11(1):83. https://doi.org/10.1186/s43088-022-00259-3

[21] Salih OS, Al-Akkam EJ. Pharmacokinetic parameters of ondansetron in rats after oral solution and transdermal invasomes gel: A comparison study. J Adv Pharm Educ Res. 2023;13(1):117. https://doi.org/10.51847/HS5a27EI6o
[22] Kachave RN, Yelmame SS, Mundhe AG. Quantitative estimation of cilnidipine and valsartan in rat plasma by RP-HPLC: its pharmacokinetic application. Futur J Pharm Sci. 2021;7:1-7. https://doi.org/10.1186/s43094-020-00153-8
[23] Shekhawat P, Pokharkar V. Risk assessment and QbD based optimization of an eprosartan mesylate nanosuspension: In-vitro characterization, PAMPA and in-vivo assessment. Int J Pharm. 2019;567:118415. https://doi.org/10.1016/j.ijpharm.2019.06.006
[24] Shariare MH, Altamimi MA, Marzan AL, Tabassum R, Jahan B, Reza HM, Rahman M, Ahsan GU, Kazi M. In vitro dissolution and bioavailability study of furosemide nanosuspension prepared using design of experiment (DoE). Saudi Pharm J. 2019;27(1):96-105. https://doi.org/10.1016/j.jsps.2018.09.002
[25] Guo X, Guo Y, Zhang M, Yang B, Liu H, Yin T, Zhang Y, He H, Wang Y, Liu D, Gou J, Tang X. A comparative study on in vitro and in vivo characteristics of enzalutamide nanocrystals versus amorphous solid dispersions and a better prediction for bioavailability based on "spring-parachute" model. Int J Pharm. 2022;628:122333. https://doi.org/10.1016/j.ijpharm.2022.122333
[26] Shinkar DM, Jadhav SS, Pingale PL, Boraste SS, VishvnathAmrutkar S. Formulation, evaluation, and optimization of glimepiride nanosuspension by using antisolvent evaporation technique. Pharmacophore. 2022;13(4):49-58. https://doi.org/10.51847/1yGT4slm1W
[27] Rajab NA , Jawad MS. Preparation and evaluation of rizatriptan benzoate loaded nanostructured lipid carrier using different surfactant/co-surfactant systems. Int J Drug Deliv Technol. 2023;13(1):120-126. http://dx.doi.org/10.25258/ijddt.13.1.18
[28] Mohammady M, Yousefi G. Freeze-drying of pharmaceutical and nutraceutical nanoparticles: The effects of formulation and technique parameters on nanoparticles characteristics. J Pharm Sci. 2020;109(11):3235-3247. https://doi.org/10.1016/j.xphs.2020.07.015
[29] Al Hazzaa SA, Rajab NA. Cilnidipine nanocrystals, formulation and evaluation for optimization of solubility and dissolution rate. Iraqi J Pharm Sci. 2023;32(Suppl.):127-135. https://doi.org/10.31351/vol32issSuppl.pp127-135
[30] Muhesen RA, Rajab NA. Formulation and characterization of olmesartan medoxomil as a nanoparticle. Res J Pharm Technol. 2023;16(7):3314-3320. https://doi.org/10.52711/0974-360X.2023.00547
[31] Mhetre RL, Hol VB, Chanshetti RR, Dhole SN. Optimisation of cilnidipine nanoparticles using box-behnken design: In-vitro, toxicity and bioavailability assessment. Mater Technol. 2022;37(11):1796-1807. http://dx.doi.org/10.1080/10667857.2021.1988038
[32] Abdulqader AA, Rajab NA. Bioavailability study of posaconazole in rats after oral poloxamer P188 nano-micelles and oral posaconazole pure drug. J Adv Pharm Educ Res. 2023;13(2):141. http://dx.doi.org/10.31351/vol32issSuppl.pp26-32
[33] Arslan A, Yet B, Nemutlu E, Akdağ Çaylı Y, Eroğlu H, Öner L. Celecoxib nanoformulations with enhanced solubility, dissolution rate, and oral bioavailability: Experimental approaches over in vitro/in vivo evaluation. Pharmaceutics. 2023;15(2):363. https://doi.org/10.3390/pharmaceutics15020363
[34] Alotaibi BS, Pervaiz F, Buabeid M, Ashames A, Fahelelbom KM, Siddique S, Shoukat H , Rehman S , Noreen S, Murtaza G. Nanostructured lipid carriers based suppository for enhanced rectal absorption of ondansetron: In vitro and in vivo evaluations. Arab J Chem. 2021;14(12):103426. https://doi.org/10.1016/j.arabjc.2021.103426
[35] Hazzaa SA, Rajab NA. A comparison study of in-vivo pharmacokinetic parameters after oral cilnidipine nanocrystals administration in rats. J Adv Pharm Educ Res. 2023;13(4):52-56. https://doi.org/10.51847/TY2pMYm8ew